THE JOURNAL OF BIOLOGICAL CHEMISTRY VOL. 287, NO. 36, pp. 30426–30435, August 31, 2012

Proteolytic Processing of Dentin Sialophosphoprotein (DSPP) Is Essential to Dentinogenesis*

Received for publication, June 5, 2012, and in revised form, July 9, 2012 Published, JBC Papers in Press, July 13, 2012, DOI 10.1074/jbc.M112.388587

Qinglin Zhu[‡§1], Monica Prasad Gibson[‡1], Qilin Liu[‡], Ying Liu[‡], Yongbo Lu[‡], Xiaofang Wang[‡], Jian Q. Feng[‡], and Chunlin Qin[‡2]

From the [‡]Department of Biomedical Sciences, Texas A&M Health Science Center, Baylor College of Dentistry, Dallas, Texas 75246 and the [§]Department of Operative Dentistry and Endodontics, The Fourth Military Medical University, School of Stomatology, Xi'an, Shaanxi 710032, China

Background: In dentin and bone, dentin sialophosphoprotein (DSPP) is processed into the NH_2-terminal and COOH-terminal fragments.
Results: The blocking of DSPP processing leads to hypomineralization defects in dentin, similar to those of *Dspp*-deficient mice.
Conclusion: The proteolytic processing of DSPP is an activation step essential to dentinogenesis.
Significance: This study represents major progress in understanding how DSPP functions in dentinogenesis.

DSPP, which plays a crucial role in dentin formation, is processed into the NH_2-terminal and COOH-terminal fragments. We believe that the proteolytic processing of DSPP is an essential activation step for its biological function in biomineralization. We tested this hypothesis by analyzing transgenic mice expressing the mutant D452A-DSPP in the *Dspp*-knock-out (*Dspp*-KO) background (referred to as "*Dspp*-KO/D452A-Tg" mice). We employed multipronged approaches to characterize the dentin of the *Dspp*-KO/D452A-Tg mice, in comparison with *Dspp*-KO mice and mice expressing the normal DSPP transgene in the *Dspp*-KO background (named *Dspp*-KO/normal-Tg mice). Our analyses showed that 90% of the D452A-DSPP in the dentin of *Dspp*-KO/D452A-Tg mice was not cleaved, indicating that D452A substitution effectively blocked the proteolytic processing of DSPP *in vivo*. While the expression of the normal DSPP fully rescued the dentin defects of the *Dspp*-KO mice, expressing the D452A-DSPP failed to do so. These results indicate that the proteolytic processing of DSPP is an activation step essential to its biological function in dentinogenesis.

Dentin sialophosphoprotein (DSPP)[3] mRNA was first identified by cDNA cloning using a mouse odontoblast cDNA library in 1997 (1). However, dentin sialoprotein (DSP) and dentin phosphoprotein (DPP), the cleaved products of the DSPP protein, were discovered much earlier and were believed to be separate entities until the single DSPP transcript was discovered (1, 2, 3). Human genetic studies have shown that *DSPP* mutations are associated with dentinogenesis imperfecta (DGI), an autosomal dominant inherited disease characterized by dentin hypomineralization and significant tooth decay (4–11). Animal studies revealed that *Dspp* knock-out (*Dspp*-KO) mice manifest hypomineralization defects in dentin. The widened predentin with irregular dentin mineralization in the *Dspp*-KO mice resembles the dentin defects of human DGI (12). These findings from human subjects and mouse models indicate that DSPP is critical for the formation and mineralization of dentin. However, the exact mechanistic steps by which DSPP functions in dentinogenesis remain largely unknown.

In dentin and bone, DSPP is proteolytically processed into the NH_2-terminal and the COOH-terminal fragments (1, 13, 14). The NH_2-terminal fragment of DSPP encoded by the 5′ portion of the DSPP transcript exists in two forms: the core protein form known as "dentin sialoprotein" (DSP) and the proteoglycan form referred to as "DSP-PG" (15–19). The COOH-terminal fragment of DSPP encoded by the 3′ region of the DSPP transcript is found in only one form, referred to as "dentin phosphoprotein" (DPP).

DSP isolated from the extracellular matrix (ECM) of rat dentin migrates at ~95 kDa on 5–15% SDS-PAGE (20). DSP accounts for 5–8% of the non-collagenous proteins (NCPS) in the ECM of rat dentin (21), while DSP-PG appears to be more abundant than DSP (15, 19). The two glycosaminoglycan (GAG) chains of DSP-PG isolated from rat dentin are made of chondroitin-4-sulfate, and the two GAG chains of mouse DSP-PG are attached to S^{242} and S^{254} in the mouse DSPP sequence (17). In porcine dentin, the DSP-PG GAG chains appear to be made of chondroitin-6-sulfate (19). DSP, which contains few or no phosphates, has no significant effect on the formation and growth of hydroxyapatite (HA) crystals according to *in vitro* mineralization analyses (22). However, information regarding the effects of DSP-PG on the formation and

* This work was supported, in whole or in part, by National Institutes of Health Grant DE005092 (to C. Q.).
[1] Both authors contributed equally to this work.
[2] To whom correspondence should be addressed: Department of Biomedical Sciences, Baylor College of Dentistry, Texas A&M Health Science Center, 3302 Gaston Ave., Dallas, TX 75246. Tel.: 214-828-8292; Fax: 214-874-4538; E-mail: cqin@bcd.tamhsc.edu.
[3] The abbreviations used are: DSPP, dentin sialophosphoprotein; *Dspp*-KO, *Dspp*-knockout; *Dspp*-KO/D452A-Tg, transgenic mouse expressing the mutant D452A-DSPP in the *Dspp*-knockout background; *Dspp*-KO/normal-Tg, transgenic mouse expressing the normal DSPP in the *Dspp*-KO background; DSP, dentin sialoprotein; DPP, dentin phosphoprotein; DGI, dentinogenesis imperfecta; DSP-PG, proteoglycan form of DSPP; ECM, extracellular matrix; NCPS, non-collagenous proteins; GAG, glycosaminoglycan; BMP1, bone morphogenetic protein 1; β-ME, β-mercaptoethanol; H&E, hematoxylin & eosin; IHC, immunohistochemistry; SEM, scanning electron microscopy; MMA, methyl-methacrylate.

growth of HA crystals is lacking. *In vivo* studies involving the transfer of a transgene encoding the NH_2-terminal fragment of DSPP into the *Dspp*-KO background indicate that this fragment might regulate the initiation of dentin mineralization but not the maturation of mineralized dentin (23).

DPP, which accounts for as much as 50% of the NCPs in the ECM of rat dentin (24), contains large amounts of aspartic acid (Asp) and serine (Ser) residues, with the majority of Ser being phosphorylated (25, 26). The Asp and phosphorylated Ser (Pse) residues are mostly present in the repeating sequences of (Asp-Pse-Pse)n and (Asp-Pse)n (1, 13, 14, 27–29). The high levels of Asp and Pse give rise to a highly phosphorylated (25) and very acidic protein with the isoelectric point estimated to be 1.1 for rat DPP (30). DPP has a relatively high affinity to calcium (31, 32) and is believed to have a direct role in controlling the rate and/or site of dentin mineralization (3, 33, 34). Several *in vitro* mineralization studies have indicated that DPP is an important initiator and modulator in the formation and growth of HA crystals (35–37).

The remarkable chemical differences between the NH_2-terminal fragment (including DSP and DSP-PG) and the COOH-terminal fragment (DPP) of DSPP suggest that these molecular variants may perform different functions in biomineralization although they are derived from the same mRNA. Studies have shown that significant amounts of DSP, DSP-PG, and DPP are present in the ECM of dentin, whereas a very minor quantity of the full-length form of DSPP is found in the dentin (16, 38). The abundance of DSPP fragments, along with the scarcity of full-length DSPP in the dentin, suggests that the processed fragments of DSPP may be the functional forms directly involved in biomineralization.

Previous *in vitro* studies by our group and others have shown that bone morphogenetic protein 1 (BMP1)/Tolloid-like metalloproteinases cleave mouse DSPP at the NH_2 terminus of Asp^{452}, while substitutions of Asp^{452} or two residues that are immediately NH_2-terminal to Asp^{452}, block the processing of this protein partially or completely (38, 39, 40). More recently, we generated transgenic mice expressing a mutant DSPP in which Asp^{452} was replaced by Ala^{452}; the transgene expressing this mutant DSPP (referred to as "D452A-DSPP") was driven by the 3.6-kb rat Col 1a1 promoter, which allows the expression of this transgene in the bone and dentin (40). We observed that the majority of D452A-DSPP was not cleaved in the bone of the transgenic mice in the wild type background, indicating that the D452A substitution effectively blocked the proteolytic processing of DSPP in the mouse bone (40). In the present study, we systematically characterized the dentin of mice expressing D452A-DSPP in the *Dspp*-KO background (referred as *Dspp*-KO/D452A-Tg mice) in comparison with *Dspp*-KO mice and mice expressing the normal DSPP transgene in the *Dspp*-KO background (named *Dspp*-KO/normal-Tg mice). Our analyses showed that 90% of the D452A-DSPP was not cleaved in the dentin of the *Dspp*-KO/D452A-Tg mice. While the expression of normal DSPP fully rescued the dentin defects of the *Dspp*-KO mice, expressing D452A-DSPP failed to do so. These results imply that the proteolytic processing of DSPP is essential to the biological function of this protein in dentinogenesis.

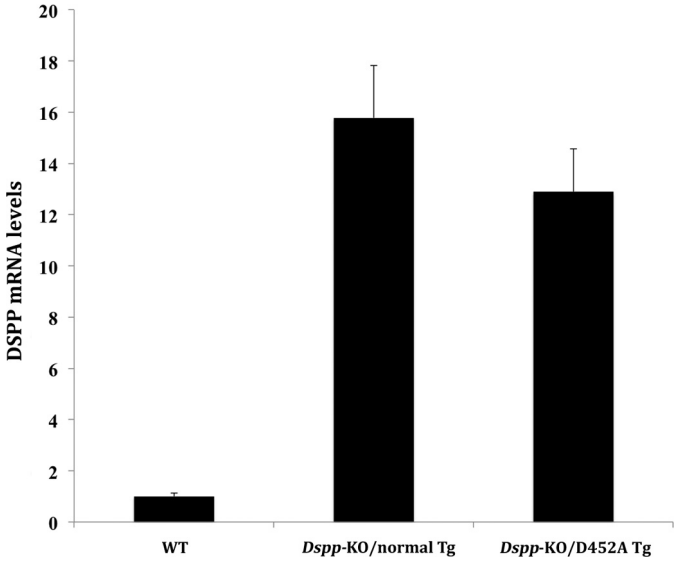

FIGURE 1. **DSPP mRNA levels in the incisor of the *Dspp*-KO/D452A-Tg and *Dspp*-KO/normal-Tg mice.** RNA isolated from the incisor of 1-month-old mice was used for real-time PCR analyses. The mRNA level in the WT mouse incisor was taken as one, while that of the *Dspp*-KO/normal-Tg or *Dspp*-KO/D452A-Tg mice was expressed as fold over the WT mice. The level of the transgenic DSPP mRNA in the *Dspp*-KO/normal-Tg mice was ~16-fold of that of the endogenous *Dspp* gene in the WT mice. The level of mRNA from the D452A-DSPP transgene in the *Dspp*-KO/D452A-Tg mice was ~13-fold of that of the endogenous *Dspp* gene in the WT mice. The forward primer sequence used for real-time PCR analysis was from exon 3 of the endogenous *Dspp* gene, while the reverse was from exon 4. The results were from five analyses ($n = 5$) for each group.

EXPERIMENTAL PROCEDURES

Generation of Dspp-KO/D452A-Tg and Dspp-KO/normal-Tg Mice—The generation of transgenic mice expressing the transgene encoding D452A-DSPP or the transgene encoding normal DSPP in the wild type (WT) background has been described in our previous report (40). In these transgenic mice, the D452A-DSPP or normal DSPP transgene is downstream to the 3.6-kb rat Col 1a1 promoter, which drives the expression of the transgenes in type I collagen-expressing tissues, including bone and dentin. The mouse lines showing the highest expression level of D452A-DSPP (*i.e.* line 4 in Zhu *et al.*, Ref. 40) or of normal DSPP (line 7 in Zhu *et al.*, Ref. 40) in the long bone were crossbred with *Dspp* knock-out (*Dspp*-KO) mice (strain name: B6; 129-Dspptm1Kul/Mmnc; MMRRC, UNC, Chapel Hill, NC). The first crossbreeding generated *Dspp*-Tg;$Dspp^{+/-}$ mice. Then, the *Dspp*-Tg;$Dspp^{+/-}$ mice were mated with $Dspp^{-/-}$ mice to generate mice expressing the D452A-DSPP or normal DSPP transgene in the *Dspp*-KO background (*i.e.* without the endogenous *Dspp* gene). The mice expressing the D452A-DSPP transgene in the *Dspp*-KO background are referred to as *Dspp*-KO/D452A-Tg mice while those expressing the normal DSPP transgene in the *Dspp*-KO background are called *Dspp*-KO/normal-Tg mice. The polymerase chain reaction (PCR) primers for detecting the DSPP transgene were: forward, 5′-CCAGTTAGTACCACTGGAAAGAGAC-3′; reverse, 5′-TCATGGTTGGTGCTATTCTTGATGC-3′ (the expected PCR products when using mouse genomic DNA as the template were 521 bp for the transgene and 676 bp for the endogenous *Dspp* gene). The primers used to identify the endogenous *Dspp* alleles were: forward, 5′-GTATCTTCATG-

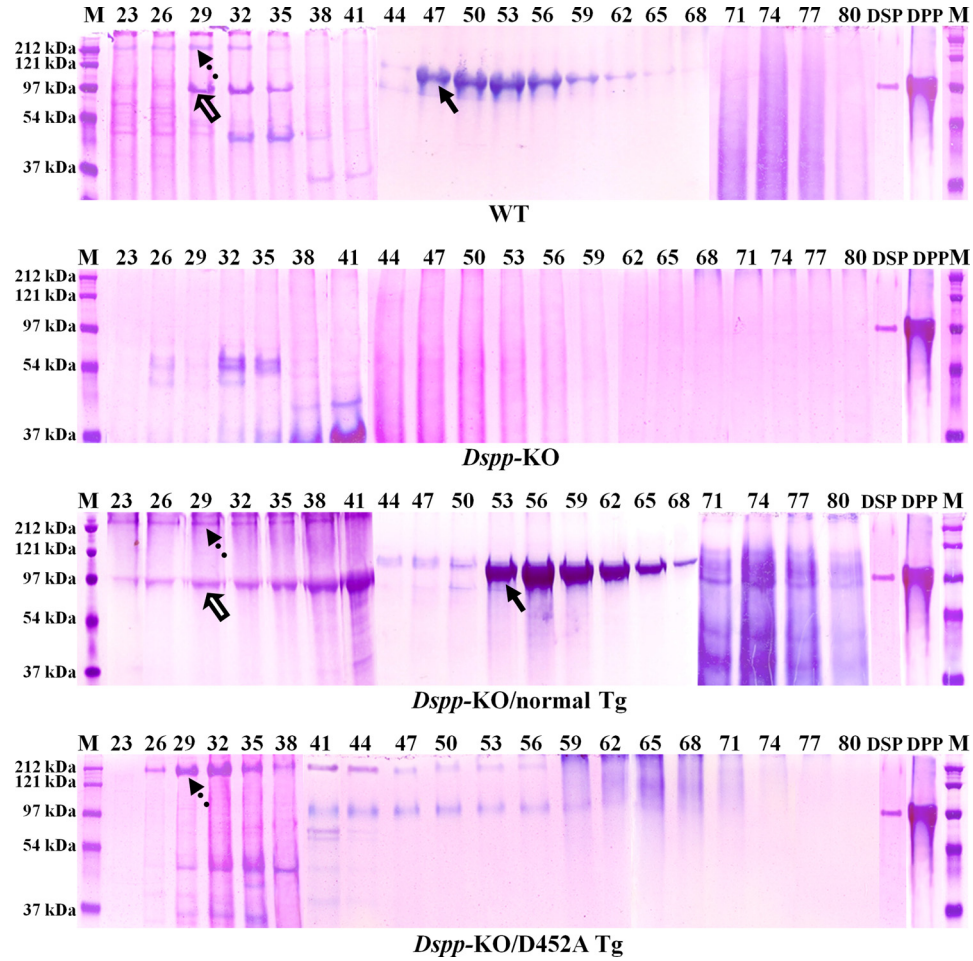

FIGURE 2. **Stains-All staining of acidic proteins (stained blue or purple) in the NCP extracts from mouse dentin.** The NCPs were extracted from the dentin of 3-month-old WT, *Dspp*-KO, *Dspp*-KO/normal-Tg and *Dspp*-KO/D452A-Tg mice. The extracted NCPs were separated into 118 fractions (0.5 ml/fraction) by a Q-Sepharose ion-exchange column; the digits on the *top* of each image represent the fraction numbers. 60 μl of sample from each of the fractions that potentially contained DSPP-derived products was loaded onto 5–15% SDS-PAGE. The *dotted arrows* denote DSPP, while the *hollow arrows* indicate DSP; their identities as DSPP and DSP were confirmed by Western immunoblotting (see Fig. 3). The major *blue bands* in fractions 47–65 in the WT and *Dspp*-KO/normal-Tg mice (*solid arrows*) was primarily made of DPP, although these bands also contained a small amount of bone sialoprotein (*BSP*), which was confirmed by anti-BSP Western immunoblotting (data not shown). It should be noted that no anti-DPP antibodies are available to detect DPP in Western immunoblotting analyses. Note the abundance of DSP and DPP in the samples from the WT and *Dspp*-KO/normal-Tg mouse incisors as well as the large amounts of full-length DSPP in the samples from the *Dspp*-KO/D452A-Tg mice. *M*, molecular weight standard; *DSP*, pure DSP isolated from rat dentin; *DPP*, pure DPP isolated from rat dentin.

GCTGTTGCTTC-3′; reverse, 5′-TGTGTTTGCCTTCATC-GAGA-3′ (expected PCR product from the endogenous *Dspp*, 489 bp). The primers specific to the *Dspp* null allele (containing *LacZ* gene) in the *Dspp*-KO mice were: forward, 5′-GTATCTTCATGGCTGTTGCTTC-3′ from the *Dspp* sequence; reverse, 5′-CCTCTTCGCTATTACGCCAG-3′ from the *LacZ* sequence (expected size of PCR product, 389 bp). The animal protocols used in this study were approved by the Animal Welfare Committee of Texas A&M Health Science Center Baylor College of Dentistry (Dallas, TX). Multiple approaches were used to characterize the mandibles of the following four types of mice: 1) *Dspp*-KO/D452A-Tg mice, 2) *Dspp*-KO/normal-Tg mice, 3) *Dspp*-KO mice, and 4) WT mice (C57/BL6J mice).

Expression Levels of the DSPP Transgenes in Teeth—Quantitative real-time PCR was performed to evaluate the relative levels of DSPP mRNA in the incisors of the 1-month-old *Dspp*-KO/D452A-Tg, *Dspp*-KO/normal-Tg and WT mice. For real-time PCR analyses, total RNA was extracted from the mouse incisors with an RNeasy mini kit (Qiagen, Germantown, MD). The RNA (1 μg/per sample) was reverse-transcripted into cDNA using the QuantiTect Rev Transcription Kit (Qiagen). The DSPP primers used for real-time PCR were: forward, 5′-AACTCTGTGGCTGTGCCTCT-3′ (in exon 3) and reverse, 5′-TATTGACTCGGAGCCATTCC-3′ (in exon 4). The real-time PCR reactions were performed as we previously reported (41).

Extraction and Isolation of Noncollagenous Proteins (NCPs) from Mouse Dentin and Detection of DSPP-related Proteins—The NCPs, including DSPP-related proteins in the dentin, were extracted from the incisors of the 3-month-old mice. Detailed protocols for the extraction of NCPs from mouse incisors have been described in our previous publications (38). The incisor extracts were separated into 118 fractions (0.5 ml/each fraction) by Q-Sepharose ion-exchange chromatography (Amersham Biosciences; Uppsala, Sweden) with a gradient ranging from 0.1 to 0.8 M NaCl in 6 M urea solution (pH 7.2). Equal amount of sample (60 ul) from each fraction were treated with

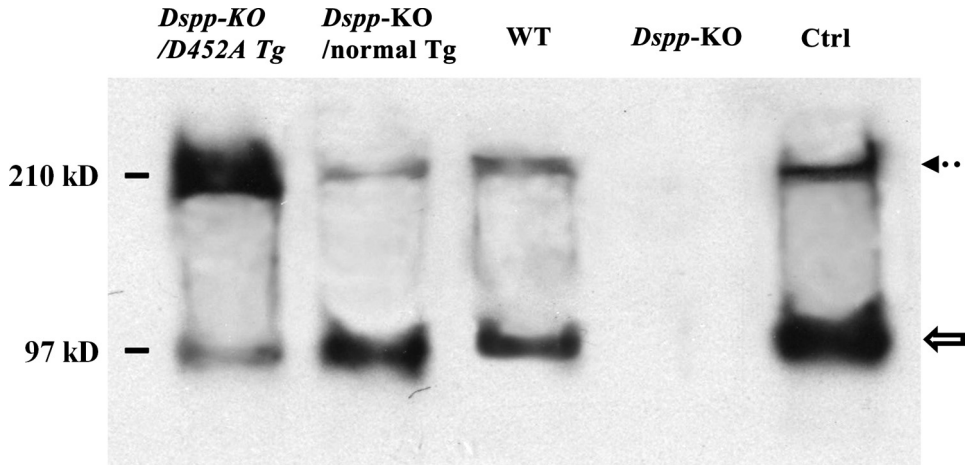

FIGURE 3. **Western immunoblotting to detect DSPP and DSP in the NCP extracts from mouse dentin.** Western immunoblotting with polyclonal anti-DSP antibodies was used to detect DSPP and DSP in the dentin extracts from the four types of mice. The partially purified rat dentin extract (0.1 μg) containing rat DSPP and DSP was used as a positive control (*Ctrl*). The Western immunoblotting results from a representative fraction (fraction 29, 60 μl) are shown here. While DSP (*hollow arrow*) and DSPP (*dotted arrow*) were detected in the dentin extracts from the *Dspp*-KO/D452A-Tg, *Dspp*-KO/normal-Tg, and WT mice, the ratios of DSP to DSPP among these three types of samples were remarkably different. Based on our integrated calculation from triplicate analyses ($n = 3$) using the image J program, we estimated that the ratio of DSP to DSPP in the *Dspp*-KO/D452A-Tg mice was 1:10, while that in the *Dspp*-KO/normal-Tg mice was 15:1. In other words, if the quantity of DSP was used for normalization, the amount of DSPP in the *Dspp*-KO/D452A-Tg mice would be ~150 times that of the full-length protein in the *Dspp*-KO/normal-Tg mice. The findings from both Stains-All and Western immunoblotting analyses showed that the D452A substitution effectively blocked the proteolytic processing of DSPP in the mouse teeth.

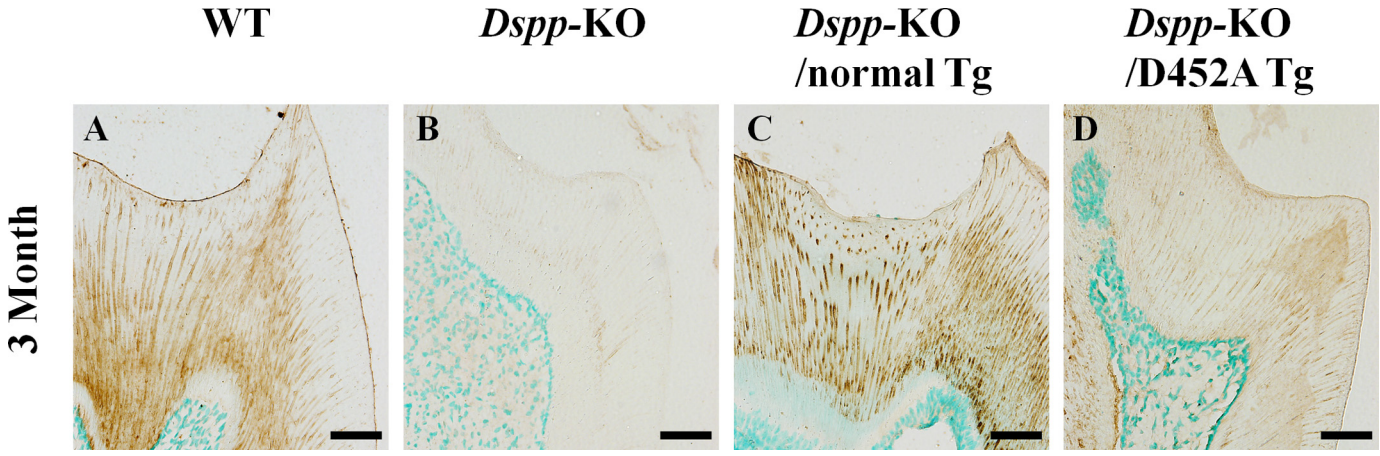

FIGURE 4. **Anti-DSP immunohistochemistry.** The specimens were from the first mandibular molars of four types of mice at postnatal 3 months. The samples from the *Dspp*-KO mice (*B*) were used as negative controls. Anti-DSP activity was observed in the dentin matrix of the WT (*A*), *Dspp*-KO/normal-Tg (*C*), and *Dspp*-KO/D452A-Tg (*D*) mice. The signal for the anti-DSP antibody in the dentin of the *Dspp*-KO/D452A-Tg mice was weaker than in the WT or *Dspp*-KO/normal-Tg mice. Bar: 50 μm.

3% β-mercaptoethanol (β-ME) and then loaded onto 5–15% SDS-PAGE. Stains-all staining was performed to visualize all the acidic NCPs in each fraction, and Western immunoblotting was used to detect the DSPP-related proteins in the fractions containing these molecules. For Western immunoblotting, we used the polyclonal anti-DSP antibody (20) at a dilution of 1:2000. Alkaline phosphatase-conjugated anti-rabbit IgG (Sigma-Aldrich) was employed as the secondary antibody for the Western immunoblotting analyses. The blots were incubated in a chemiluminescent substrate CDP-star (Ambion, Austin, TX) for 5 min and exposed to x-ray films. The image J software program was employed to scan the positive bands and measure their densities and areas for calculating the ratio of DSP to DSPP in each analysis.

Plain X-ray Radiography and Micro-computed Tomography (μ-CT)—The mandibles from the 3-month-old and 6-month-old mice were dissected from the four groups of mice and analyzed with the Faxitron MX-20 Specimen Radiography System (Faxitron x-ray Corp., Buffalo Grove, IL). For the μ-CT analyses, the mandibles were scanned using μ-CT35 imaging system (Scanco Medical, Basserdorf, Switzerland), as we previously described (42). In the μ-CT program, a scan of the whole mandible in 7.0-μm slice increments was selected for three-dimensional reconstructions to assess the shape and structure of the mouse mandibles.

Histology and Immunohistochemistry—Under anesthesia, the *Dspp*-KO/D452A-Tg, *Dspp*-KO/normal-Tg, *Dspp*-KO and WT mice at the ages of postnatal 3 and 6 months were perfused from the ascending aorta with 4% paraformaldehyde in 0.1 M phosphate buffer. The mandibles were dissected and further fixed in the same fixative for 24 h, and then decalcified in 8% EDTA containing 0.18 M sucrose (pH 7.4) at 4 °C for approximately 2 weeks. The tissues were subsequently processed for paraffin embedding, and serial sections of 5 μm were prepared.

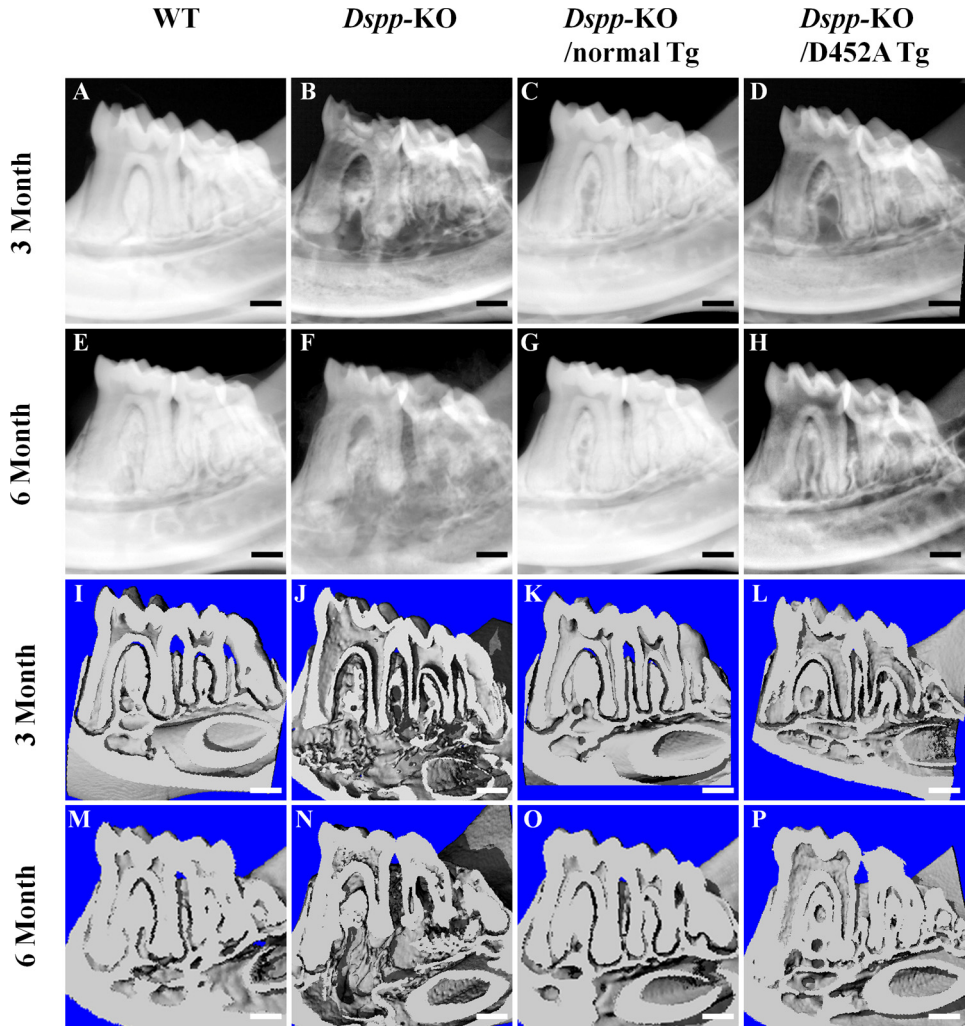

FIGURE 5. **Plain x-ray analyses (*A–H*) and the μ-CT analyses (*I–P*) of mandibles from 3- and 6-month-old mice.** At postnatal 3 months, the WT mice had evenly distributed and well mineralized dentin (*A*). The mandibular molars in the *Dspp*-KO mice (*B*) had an enlarged pulp chamber and thinner dentin compared with the WT mice. The tooth defects in the *Dspp*-KO/D452A-Tg mice (*D*) were similar to those of the *Dspp*-KO mice, whereas the teeth of the *Dspp*-KO/normal-Tg mice (*C*) resembled those of the WT mice. At postnatal 6 months, the teeth in the *Dspp*-KO/normal-Tg mice (*G*) also appeared the same as those in the WT mice (*E*), while the teeth of the *Dspp*-KO/D452A-Tg mice (*H*) resembled the *Dspp*-KO mouse teeth (*F*). In the μ-CT analyses of mandibles, the teeth of the *Dspp*-KO (*J*, *N*) and *Dspp*-KO/D452A-Tg (*L*, *P*) mice had similar dental defects, which included enlarged pulp chambers and thinner dentin. The WT (*I*, *M*) and *Dspp*-KO/normal-Tg (*K*, *O*) mice had normal dental structures. Bar: 200 μm.

The sections were either stained with hematoxylin & eosin (H&E) or used for immunohistochemistry (IHC) analyses. For the IHC analyses, the anti-DSP-2C12.3 monoclonal antibody (43) was used at a dilution of 1:800 to detect DSPP and DSP. The anti-biglycan antibody (a gift from Dr. Larry Fisher of the Craniofacial and Skeletal Diseases Branch, National Institutes of Health, Bethesda, MD) was used at a 1:1000 dilution to detect biglycan. Mouse IgG of the same concentration as that of the primary antibody was the negative control. All the IHC experiments were carried out using the M.O.M. kit and DAB kit (Vector Laboratories; Burlingame, CA) according to the manufacturer's instructions.

Backscattered and Resin-casted Scanning Electron Microscopy (SEM)—The dissected mandibles were fixed in 2% paraformaldehyde and 2.5% glutaraldehyde in 0.1 M cacodylate buffer solution (pH 7.4) at room temperature. Four hours later, the fixation buffer was replaced with 0.1 M cacodylate solution. The specimens were then dehydrated in ascending concentrations of ethanol and embedded in methyl-methacrylate (MMA) resin (Buehler, Lake Bluff, IL). The surfaces of the dentin tissues of interest were polished using a micro cloth with Metadi Supreme Polycrystalline diamond suspensions of decreasing sizes (0.1 μm, 0.25 μm, and 0.05 μm; Buehler, Lake Bluff, IL). The samples were then washed in the ultrasonic wash and placed in the vacuum system overnight. For backscattered SEM, the surfaces of the teeth embedded in MMA were polished and coated with carbon. For the resin- casted SEM, the dentin surface was acid etched with 37% phosphoric acid for 2–10 s and washed with 5.25% sodium hypochlorite for 5 min. The samples were then coated with gold and palladium as described previously (44). A FEI/Philips XL30 Field emission environmental SEM (Philips, Hillsboro, OR) was used to perform the SE analyses.

Double Fluorochrome Labeling of the Dentin—Double fluorescence labeling was performed, as we described previously, to analyze the mineral deposition rate of the dentin in the mouse incisors (42, 45). Briefly, calcein (green) label (Sigma Aldrich) was injected into the abdominal cavities of the 5-week-old mice

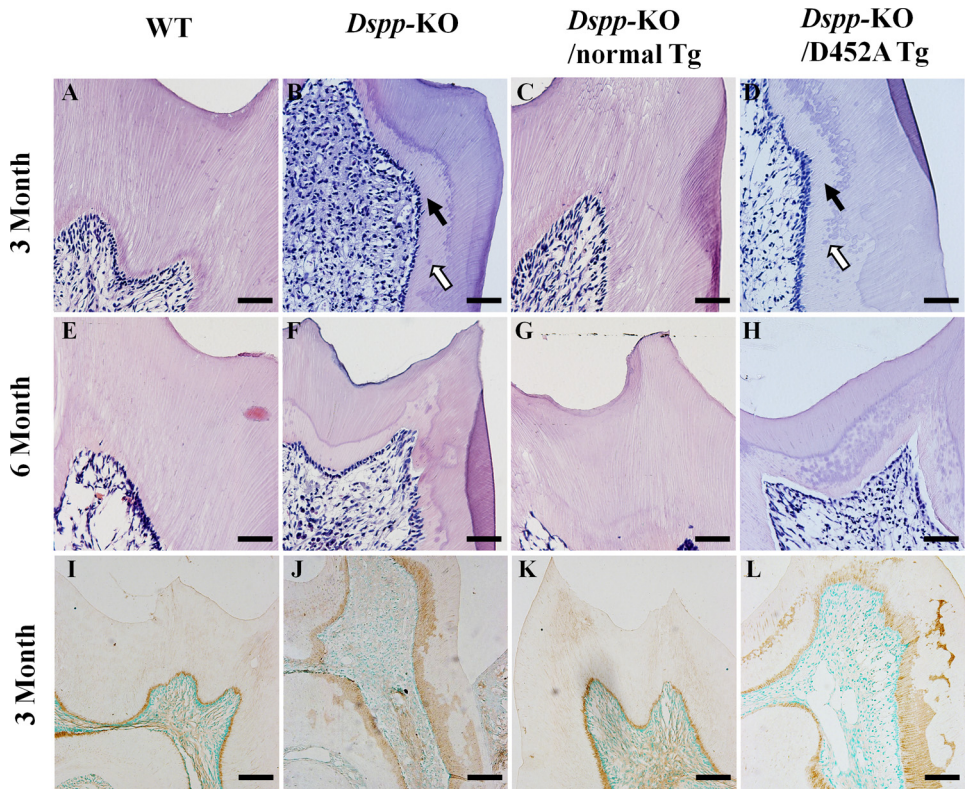

FIGURE 6. **H&E staining of the dentin-pulp complex in 3- and 6-month-old mice (*A–H*) and biglycan immunostaining of predentin/dentin in 3-month-old mice (*I–L*).** At postnatal 3 months, the *Dspp*-KO mice (*B*) had wider predentin (*solid arrow*), uncoalescent calcospherites (*hollow arrow*) and an irregular dentin-predentin border compared with the WT mice (*A*). The *Dspp*-KO/D452A-Tg mice (*D*) showed dentin abnormalities similar to those of the *Dspp*-KO mice (*B*). The dentin of the *Dspp*-KO/normal-Tg (*C*) mice resembled that of the WT mice (*A*). At postnatal 6 months, the dentin-pulp structures in the *Dspp*-KO/normal-Tg (*G*) mice resembled those of the WT mice (*E*), while the *Dspp*-KO/D452A-Tg mouse teeth (*H*) resembled those of the *Dspp*-KO mice (*F*). Bar: *A–H* = 50 μm. In the biglycan immunostaining of predentin/dentin, the predentin stained by the anti-biglycan antibody (*brown color*) in the WT mice (*I*) and *Dspp*-KO/normal-Tg mice (*K*) was thin, smooth and evenly distributed, while the predentin in the *Dspp*-KO mice (*J*) and *Dspp*-KO/D452A-Tg mice (*L*) was wider and unevenly distributed. Bar: *I–L* = 100 μm.

at 5 mg/kg. One week later, 20 mg/kg of Alizarin Red label (Sigma Aldrich) was administered intraperitoneally. The mice were sacrificed 48 h after the injection of Alizarin Red label. The mandibles were dissected and fixed in 70% ethanol for 48 h and dehydrated through ascending concentrations of ethanol (70–100%) and embedded in MMA. Sections (10 μm thick) were cut and viewed under epifluorescent illumination using a Nikon E800 microscope interfaced with Osteomeasure histomorphometry software (version 4.1, Atlanta, GA). The distance between the two fluorescence labels of the incisor dentin (cross section of incisors under the mesial root of the first molar) was determined, averaged and divided by seven to calculate the mineral deposition rate, expressed as μm/day.

RESULTS

The dentin and bone of the transgenic mice expressing the normal DSPP transgene or the D452A-DSPP transgene in the wild type background were the same as those of normal mice. In the following section, we describe in detail the dentin phenotypes of the *Dspp*-KO/D452A-Tg mice and *Dspp*-KO/normal-Tg mice in comparison with the *Dspp*-KO mice and WT mice. We noticed that the *Dspp*-KO and *Dspp*-KO/D452A-Tg mice also had alveolar bone defects. In this report, we did not include a description of the non-dentin defects in these *Dspp*-mutant mice.

Expression of the DSPP Transgenes in the Teeth—Real-time PCR analyses using the mouse incisor RNA as the template revealed that the expression level of the normal DSPP transgene in the *Dspp*-KO background was ~16-fold of the transcription level of the endogenous *Dspp* in the WT mice, while the expression level of D452A-DSPP transgene was about 13-fold of the endogenous *Dspp* in the WT mice (Fig. 1).

Extraction and Separation of NCPs and Detection of DSPP-related Proteins—Stains-All staining and Western immunoblotting were used to visualize the DSPP-derived proteins in the dentin of the *Dspp*-KO/D452A-Tg, *Dspp*-KO/normal-Tg, and WT mice. All the chromatographic fractions from the dentin extracts that might contain DSPP-related products were analyzed by SDS-PAGE with Stains-All staining (Fig. 2). In the extracts from the WT and *Dspp*-KO/normal-Tg mouse incisors, DSP (Fig. 2, *hollow arrows*) was clearly visualized by Stains-All, along with weak protein bands matching the migration rate of full-length DSPP (Fig. 2, *dotted arrows*). While large amounts of the full-length DSPP were observed in the *Dspp*-KO/D452A-Tg mice, protein bands matching the DSP were hardly detectable in the incisors of these mice. In the *Dspp*-null mice, no DSPP-related signals were observed.

In the Western immunoblotting analyses, DSP and DSPP were clearly detected in the dentin extracts from the WT, *Dspp*-

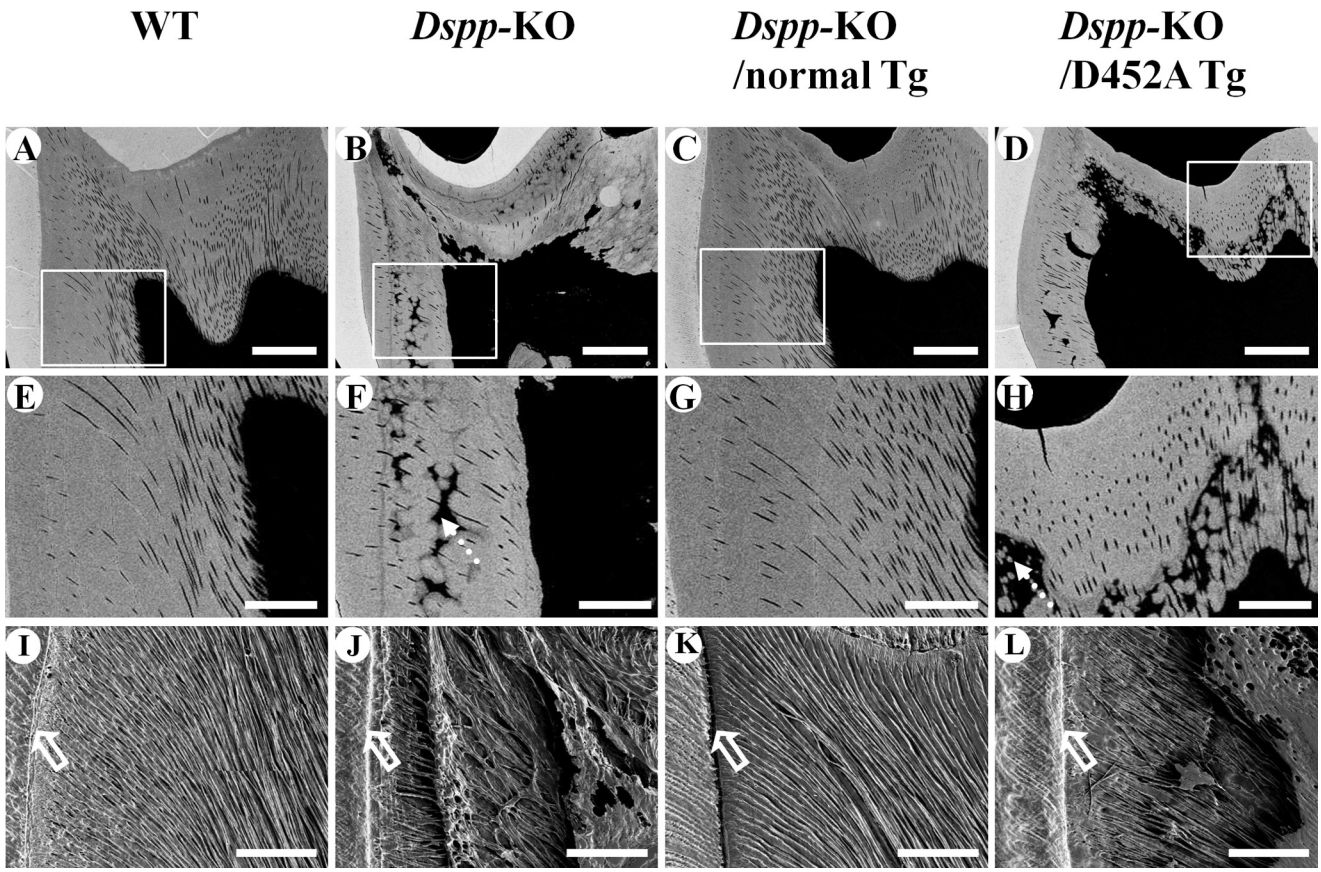

FIGURE 7. **Backscattered SEM analyses (*A–H*) and resin infiltration and acid-etched SEM analyses (*I–L*) of the mandibular first molar from 3-month-old mice.** In the backscattered SEM images, the *white areas* represent the regions with greater amounts of mineral (higher level of mineralization), while the *black areas* indicate those with less mineral (lower level of mineralization). The dentin in the *Dspp*-KO (*B*, *F*) and *Dspp*-KO/D452A-Tg mice (*D*, *H*) had more *black areas* (*dotted arrows*) than in the WT (*A*, *E*) or *Dspp-KO*/normal-Tg (*C*, *G*) mice, indicating that the former two had more hypomineralized areas than in the latter two. The images in *E–H* are enlarged views of the *boxed areas* in *A–D*. Bar: A-D = 100 μm, *E–H* = 40 μm. In the resin infiltration and acid-etched SEM images of the mandibular first molar, the dentinal tubules in the WT mice (*I*) and *Dspp*-KO/normal-Tg mice (*K*) had uniform diameters and were evenly distributed, running parallel to each other and perpendicular to the dental enamel junction (*DEJ*, *hollow arrows*). In contrast, the dentinal tubules in the *Dspp*-KO (*J*) and *Dspp*-KO/D452A-Tg (*L*) mice were tangled, had uneven diameters, and appeared collapsed. Bar: *I–L* = 50 μm.

KO/D452A-Tg and *Dspp*-KO/normal-Tg mice (Fig. 3). The ratios of DSP (hollow arrow) to DSPP (dotted arrow) varied dramatically between the samples from the *Dspp*-KO/D452A-Tg mice and the *Dspp*-KO/normal-Tg mice. The ratio of DSP to DSPP in the *Dspp*-KO/D452A-Tg mice was 1:10, while that in the *Dspp*-KO/normal-Tg mice was 15:1, indicating that the full-length form of DSPP in the former mice was ~150-fold greater than in the latter. The findings from both the Stains-All and Western immunoblotting analyses indicate that D452A substitution effectively blocked the proteolytic processing of DSPP in the mouse teeth.

Anti-DSP Immunostaining—Anti-DSP reactivity was observed in the odontoblasts and the dentin matrix of the WT, *Dspp*-KO/D452A-Tg, and *Dspp*-KO/normal-Tg mice (Fig. 4). In the matrix, the anti-DSP signals were primarily detected around the dentinal tubules in both the *Dspp*-KO/normal-Tg mice (Fig. 4*C*) and *Dspp*-KO/D452A-Tg mice (Fig. 4*D*). The presence of anti-DSP activity in the dentin matrix of the *Dspp*-KO/D452A-Tg mice indicated that the uncleaved DSPP, like its processed fragments, was also secreted into the ECM (Fig. 4*D*).

Plain X-ray and μ-CT Analyses—Plain x-ray radiography (Fig. 5, *A–H*) and μ-CT (Fig. 5, *I–P*) analyses were performed to reveal the dentin structure in the 3- and 6-month-old mice. These analyses showed enlarged pulp chambers with very thin dentin in the *Dspp*-KO mice (Fig. 5, *B*, *F*, *J*, and *N*). The expression of normal DSPP transgene fully rescued the defects of enlarged pulp and thin dentin in the *Dspp* KO mice (Fig. 5, *C*, *G*, *K*, and *O*), whereas the D452A-DSPP transgene failed to reverse the dentin defects of the *Dspp*-KO mice (Fig. 5, *D*, *H*, *L*, and *P*).

Histological Analysis—At postnatal 3 and 6 months, the pulp chamber in the mandibular molars of the *Dspp*-KO mice was remarkably larger and the predentin zone was much wider than in the WT mice (Fig. 6, *A*, *B*, *E*, and *F*). While the structure of the dentin-pulp complex in the *Dspp*-KO/normal-Tg mice (Fig. 6, *C* and *G*) was similar to that of the WT mice, the structure of the *Dspp*-KO/D452A-Tg mice (Fig. 6, *D* and *H*) resembled the one in the *Dspp*-KO mice. The histology findings confirmed x-ray data showing that the normal DSPP transgene rescued the *Dspp*-KO dentin defects while the mutant transgene did not.

Anti-biglycan Immunostaining—Biglycan immunostaining (Fig. 6, *I–L*) was performed to show the predentin zone since in the teeth, this proteoglycan is primarily localized in the predentin. The biglycan immunostaining analyses clearly showed that the predentin zone in the *Dspp*-KO (Fig. 6*J*) and *Dspp*-KO/D452A-Tg mice (Fig. 6*L*) was much wider and more irregular

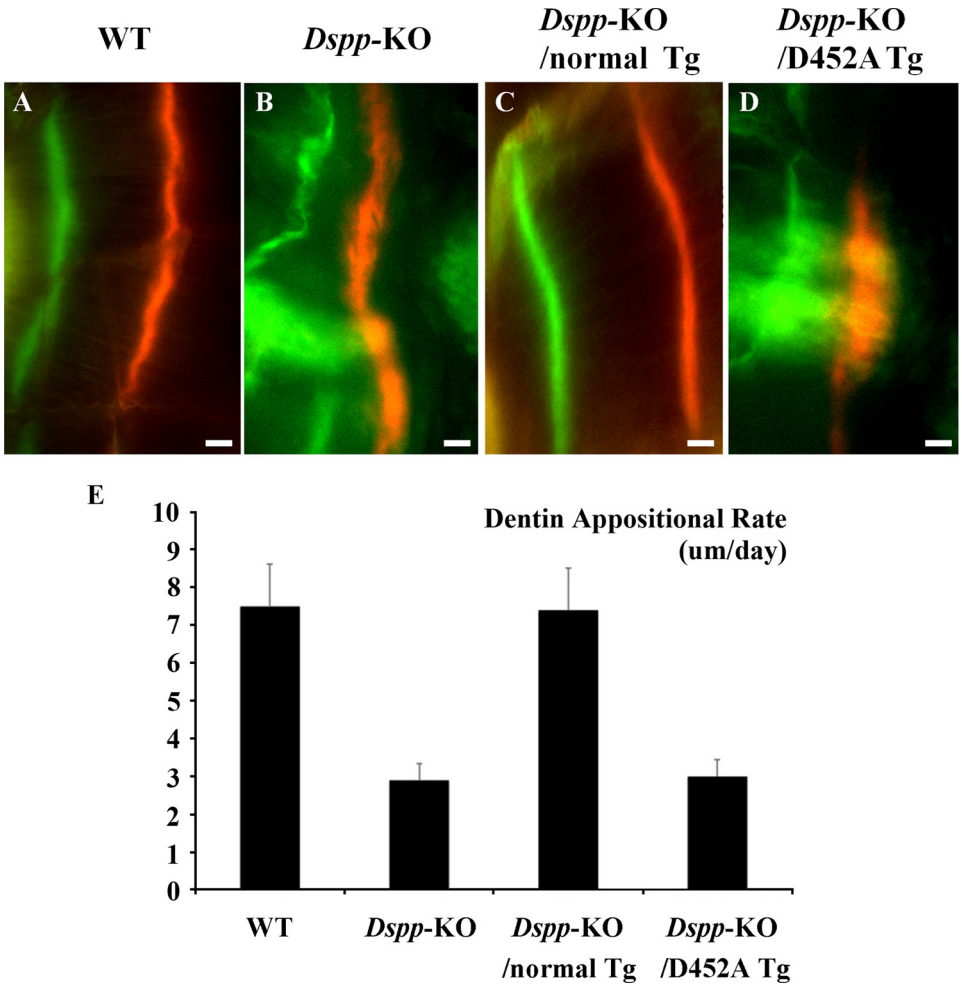

FIGURE 8. **Double fluorochrome labeling.** The specimens were from the dentin of 5-week-old WT (*A*), *Dspp*-KO (*B*), *Dspp*-KO/normal-Tg mice (*C*), and *Dspp*-KO/D452A-Tg mice (*D*). In these analyses, the first injection (calcein) produced a *green label*, while the second injection (Alizarin Red) made a *red label*. The distance between the green zone and the red zone reflected the width of the dentin matrix that was mineralized in 7 days. Compared with the normal dentin in the WT and *Dspp*-KO/normal-Tg mice, the labeling zones in the *Dspp*-KO mice and *Dspp*-KO/D452A-Tg mice were diffused, indicating an irregular deposition of mineral. Bars = 10 μm. *E*, quantitative analyses ($n = 3$) showed that the dentin of the *Dspp*-KO mice and *Dspp*-KO/D452A-Tg mice had a remarkably lower mineral deposition rate compared with the WT and *Dspp*-KO/normal-Tg mice.

than that in the WT (Fig. 6*I*) or *Dspp*-KO/normal-Tg mice (Fig. 6*K*).

Backscattered SEM—Backscattered SEM analyses (Fig. 7, *A–H*) indicated that the dentin in the *Dspp*-KO mice (Fig. 7, *B* and *F*) and *Dspp*-KO/D452A-Tg mice (Fig. 7, *D* and *H*) contained more areas that were unmineralized or hypomineralized and resembled interglobular dentin. In the backscattered SEM images, the white areas represent the regions with greater amounts of mineral (higher level of mineralization), while the black areas indicate less mineralization (*i.e.* unmineralized or hypomineralized). The dentin in the *Dspp*-KO (Fig. 7, *B* and *F*) and *Dspp*-KO/D452A-Tg mice (Fig. 7, *D* and *H*) contained more hypomineralized areas compared with the WT (Fig. 7, *A* and *E*) and *Dspp*-KO/normal-Tg (Fig. 7, *C* and *G*) mice.

Resin-casted SE—The resin-casted SE analyses (Fig. 7, *I–L*) revealed that the dentin in the WT (Fig. 7*I*) and *Dspp*-KO/normal-Tg mice (Fig. 7*K*) had well organized and evenly distributed dentinal tubules of similar thickness, whereas in the *Dspp*-KO (Fig. 7*J*) and *Dspp*-KO/D452A-Tg (Fig. 7*L*) mice, the dentinal tubules were disorganized and collapsed in some areas.

Double Fluorochrome Labeling—In the WT (Fig. 8*A*) and *Dspp*-KO/normal-Tg mice (Fig. 8*C*), the two labeled zones were regular and evenly distributed. In the *Dspp*-KO (Fig. 8*B*) and *Dspp*-KO/D452A-Tg mice (Fig. 8*D*), the zones of fluorochrome labeling appeared irregular and diffused; in certain areas, the boundary between the two labels appeared blurry. In the double fluorochrome labeling analyses, the distance between the green (first) labeling and red (second) labeling represented the mineral deposition of the dentin matrix during the period between the two injections (7 days). The quantitative analyses of the distance between the two labels (Fig. 8*E*) indicated that the mineral deposition rates in the dentin of the *Dspp*-KO and *Dspp*-KO/D452A-Tg mice were much lower than in the WT or *Dspp*-KO/normal-Tg mice.

DISCUSSION

In the ECM of dentin and bone, DSPP is mainly present as the processed NH_2-terminal and COOH-terminal fragments (including DSP, DSP-PG, and DPP); only a minor amount of full-length DSPP could be detected in the dentin of wild type rat

or mouse (38). Based on the abundance of DSPP fragments and scarcity of its full-length form in the dentin, along with the observed roles of DPP in the nucleation and modulation of apatite crystal formation, we hypothesized that the conversion of DSPP to its fragments by proteolytic processing may be an activation event, converting an inactive precursor to active forms, and this activation step may represent one of the controlling mechanisms in dentin formation (16, 40, 46). In this study, we generated *Dspp*-KO/D452A-Tg mice lacking the endogenous *Dspp* gene but expressing the transgenic D452A-DSPP protein, in which Asp^{452}, a key cleavage-site residue, was replaced by Ala^{452}. The dentin of the *Dspp*-KO/D452A-Tg mice was compared with that of the *Dspp*-KO mice, WT mice and *Dspp*-KO/normal-Tg mice that lacked the endogenous *Dspp* gene but expressed the transgenic expression of normal DSPP protein. These analyses showed that the D452A substitution effectively blocked the proteolytic processing of this protein in dentin and led to the inactivation of this molecule in dentinogenesis. The findings in the present investigation lend strong support to our hypothesis that the proteolytic processing of DSPP is an activation event, essential to its biological function in biomineralization.

A small portion (10%) of D452A-DSPP was cleaved in the *Dspp*-KO/D452A-Tg mice. Previously, we showed that substitutions of Asp^{452} and other residues close to this residue could not totally block the cleavage of DSPP by BMP1 *in vitro*, suggesting the presence of a secondary (cryptic) cleavage site that is currently unidentified (40). Nevertheless, the dentin defects in the *Dspp*-KO/D452A-Tg mice were very similar to those in the *Dspp*-KO mice; this observation indicates that the cleavage of DSPP at this cryptic cleavage site has a very limited effect on DSPP activation.

Immunohistochemistry with the monoclonal anti-DSP antibody revealed positive signals for DSP in the dentin matrix of the *Dspp*-KO/D452A-Tg mice, indicating that the uncleaved full-length DSPP was also secreted into the ECM of dentin. The anti-DSP activity in the dentin of the *Dspp*-KO/D452A-Tg mice was weaker than in the *Dspp*-KO/normal-Tg mice or WT mice. The relatively weaker signal for the anti-DSP antibody in the dentin of the *Dspp*-KO/D452A-Tg mice may be attributed to the difference in the degree of exposure of the epitopes (antigenic determinants); *i.e.* the epitopes of the processed fragment (DSP) may be more easily exposed and readily recognized by the anti-DSP antibody than the same antigenic determinants wrapped up in the full-length form of DSPP.

In addition to dentin and bone, DSPP has also been found in certain soft tissues such as the salivary glands, cartilage, liver, kidney, and brain (41, 47). It appears that the DSPP-derived products in the non-mineralized tissues may have posttranslational modifications different from those in the dentin. For example, the majority of DSPP in the condylar cartilage was not cleaved (47), and DSP in the non-mineralized tissues may be devoid of any carbohydrate moieties (41). These variations in the posttranslational modifications of DSPP suggest that the biological role of DSPP in the non-mineralized tissue might differ from that in dentin and bone, in which the cleavage of the full-length protein into its fragment forms is essential to its biological function in the mineralization of these two tissues.

Acknowledgments—We thank Jeanne Santa Cruz for assistance with the editing of this article, and Dr. Paul Dechow for support with the micro-CT analyses.

REFERENCES

1. MacDougall, M., Simmons, D., Luan, X., Nydegger, J., Feng, J., and Gu, T. T. (1997) Dentin phosphoprotein and dentin sialoprotein are cleavage products expressed from a single transcript coded by a gene on human chromosome 4. Dentin phosphoprotein DNA sequence determination. *J. Biol. Chem.* **272,** 835–842
2. Butler, W. T., Bhown, M., Dimuzio, M. T., and Linde, A. (1981) Nonocollagenous proteins of dentin. Isolation and partial characterization of rat dentin proteins and proteoglycans using a three-step preparative method. *Coll. Relat. Res.* **1,** 187–199
3. Veis, A., and Perry, A. (1967) The phosphoprotein of the dentin matrix. *Biochemistry* **6,** 2409–2416
4. Xiao, S., Yu, C., Chou, X., Yuan, W., Wang, Y., Bu, L., Fu, G., Qian, M., Yang, J., Shi, Y., Hu, L., Han, B., Wang, Z., Huang, W., Liu, J., Chen, Z., Zhao, G., and Kong, X. (2001) Dentinogenesis imperfecta 1 with or without progressive hearing loss is associated with distinct mutations in DSPP. *Nat. Genet.* **27,** 201–204
5. Zhang, X., Zhao, J., Li, C., Gao, S., Qiu, C., Liu, P., Wu, G., Qiang, B., Lo, W. H., and Shen, Y. (2001) DSPP mutation in dentinogenesis imperfecta Shields type II. *Nat. Genet.* **27,** 151–152
6. Kim, J. W., and Simmer, J. P. (2007) Hereditary dentin defects. *J. Dent. Res.* **86,** 392–399
7. Holappa, H., Nieminen, P., Tolva, L., Lukinmaa, P. L., and Alaluusua, S. (2006) Splicing site mutations in dentin sialophosphoprotein causing dentinogenesis imperfecta type II. *Eur. J. Oral. Sci.* **114,** 381–384
8. Malmgren, B., Lindskog, S., Elgadi, A., and Norgren, S. (2004) Clinical, histopathologic, and genetic investigation in two large families with dentinogenesis imperfecta type II. *Hum. Genet.* **114,** 491–498
9. Rajpar, M. H., Koch, M. J., Davies, R. M., Mellody, K. T., Kielty, C. M., and Dixon, M. J. (2002) Mutation of the signal peptide region of the bicistronic gene DSPP affects translocation to the endoplasmic reticulum and results in defective dentine biomineralization. *Hum. Mol. Genet.* **11,** 2559–2565
10. Kim, J. W., Nam, S. H., Jang, K. T., Lee, S. H., Kim, C. C., Hahn, S. H., Hu, J. C., and Simmer, J. P. (2004) A novel splice acceptor mutation in the DSPP gene causing dentinogenesis imperfecta type II. *Hum. Genet.* **115,** 248–254
11. Dong, J., Gu, T., Jeffords, L., and MacDougall, M. (2005) Dentin phosphoprotein compound mutation in dentin sialophosphoprotein causes dentinogenesis imperfecta type III. *Am. J. Med. Genet. A* **132A,** 305–309
12. Sreenath, T., Thyagarajan, T., Hall, B., Longenecker, G., D'Souza, R., Hong, S., Wright, J. T., MacDougall, M., Sauk, J., and Kulkarni, A. B. (2003) Dentin sialophosphoprotein knockout mouse teeth display widened predentin zone and develop defective dentin mineralization similar to human dentinogenesis imperfecta type III. *J. Biol. Chem.* **278,** 24874–24880
13. Ritchie, H. H., Wang, L. H., and Knudtson, K. (2001) A novel rat 523 amino acid phosphophoryn: nucleotide sequence and genomic organization. *Biochim. Biophys. Acta* **1520,** 212–222
14. Gu, K., Chang, S., Ritchie, H. H., Clarkson, B. H., and Rutherford, R. B. (2000) Molecular cloning of a human dentin sialophosphoprotein gene. *Eur. J. Oral. Sci.* **108,** 35–42
15. Qin, C., Brunn, J. C., Baba, O., Wygant, J. N., McIntyre, B. W., and Butler, W. T. (2003) Dentin sialoprotein isoforms: detection and characterization of a high molecular weight dentin sialoprotein. *Eur. J. Oral. Sci.* **111,** 235–242
16. Prasad, M., Butler, W. T., and Qin, C. (2010) Dentin sialophosphoprotein in biomineralization. *Connect. Tissue Res.* **51,** 404–417
17. Zhu, Q., Sun, Y., Prasad, M., Wang, X., Yamoah, A. K., Li, Y., Feng, J., and Qin, C. (2010) Glycosaminoglycan chain of dentin sialoprotein proteoglycan. *J. Dent. Res.* **89,** 808–812
18. Sugars, R. V., Olsson, M. L., Waddington, R., and Wendel, M. (2006) Substitution of bovine dentine sialoprotein with chondroitin sulfate glycosaminoglycan chains. *Eur. J. Oral. Sci.* **114,** 89–92

19. Yamakoshi, Y., Hu, J. C., Fukae, M., Iwata, T., Kim, J. W., Zhang, H., and Simmer, J. P. (2005) Porcine dentin sialoprotein is a proteoglycan with glycosaminoglycan chains containing chondroitin 6-sulfate. *J. Biol. Chem.* **280,** 1552–1560
20. Butler, W. T., Bhown, M., Brunn, J. C., D'Souza, R. N., Farach-Carson, M. C., Happonen, R. P., Schrohenloher, R. E., Seyer, J. M., Somerman, M. J., and Foster, R. A. (1992) Isolation, characterization and immunolocalization of a 53-kDal dentin sialoprotein (DSP). *Matrix* **12,** 343–351
21. Butler, W. T. (1995) Dentin matrix proteins and dentinogenesis. *Connect. Tissue Res.* **33,** 59–65
22. Boskey, A., Spevak, L., Tan, M., Doty, S. B., and Butler, W. T. (2000) Dentin sialoprotein (DSP) has limited effects on *in vitro* apatite formation and growth. *Calcif. Tissue. Int.* **67,** 472–478
23. Suzuki, S., Sreenath, T., Haruyama, N., Honeycutt, C., Terse, A., Cho, A., Kohler, T., Muller, R., Goldberg, M., and Kulkarni, A. B. (2009) Dentin sialoprotein and dentin phosphoprotein have distinct roles in dentin mineralization. *Matrix Biol.* **28,** 221–229
24. MacDougall, M., Zeichner-David, M., and Slavkin, H. C. (1985) Production and characterization of antibodies against murine dentine phosphoprotein. *Biochem. J.* **232,** 493–500
25. Butler, W. T., Bhown, M., DiMuzio, M. T., Cothran, W. C., and Linde, A. (1983) Multiple forms of rat dentin phosphoproteins. *Arch Biochem. Biophys.* **225,** 178–186
26. Lee, S. L., Veis, A., and Glonek, T. (1977) Dentin phosphoprotein: an extracellular calcium-binding protein. *Biochemistry* **16,** 2971–2979
27. Butler, W. T., Brunn, J. C., and Qin, C. (2003) Dentin extracellular matrix (ECM) proteins: comparison to bone ECM and contribution to dynamics of dentinogenesis. *Connect. Tissue Res.* **44,** 171–178
28. George, A., Bannon, L., Sabsay, B., Dillon, J. W., Malone, J., Veis, A., Jenkins, N. A., Gilbert, D. J., and Copeland, N. G. (1996) The carboxyl-terminal domain of phosphophoryn contains unique extended triplet amino acid repeat sequences forming ordered carboxyl-phosphate interaction ridges that may be essential in the biomineralization process. *J. Biol. Chem.* **271,** 32869–32873
29. Ritchie, H. H., and Wang, L. H. (1996) Sequence determination of an extremely acidic rat dentin phosphoprotein. *J. Biol. Chem.* **271,** 21695–21698
30. Jonsson, M., and Fredriksson, S. (1978) Isoelectric focusing of the phosphoprotein of rat-incisor dentin in ampholine and acid pH gradients. Evidence for carrier ampholyte-protein complexes. *J. Chromatogr.* **157,** 234–242
31. Zanetti, M., de Bernard, B., Jontell, M., and Linde, A. (1981) Ca^{2+}-binding studies of the phosphoprotein from rat-incisor dentine. *Eur. J. Biochem.* **113,** 541–545
32. Marsh, M. E. (1989) Binding of calcium and phosphate ions to dentin phosphophoryn. *Biochemistry* **28,** 346–352
33. Dickson, I. R., Dimuzio, M. T., Volpin, D., Ananthanarayanan, S., and Veis, A. (1975) The extraction of phosphoproteins from bovine dentin. *Calcif. Tissue Res.* **19,** 51–61
34. Dimuzio, M. T., and Veis, A. (1978) The biosynthesis of phosphophoryns and dentin collagen in the continuously erupting rat incisor. *J. Biol. Chem.* **253,** 6845–6852
35. Linde, A. (1989) Dentin matrix proteins: composition and possible functions in calcification. *Anat. Rec.* **224,** 154–166
36. Boskey, A. L., Maresca, M., Doty, S., Sabsay, B., and Veis, A. (1990) Concentration-dependent effects of dentin phosphophoryn in the regulation of in vitro hydroxyapatite formation and growth. *Bone Miner* **11,** 55–65
37. Saito, T., Arsenault, A. L., Yamauchi, M., Kuboki, Y., and Crenshaw, M. A. (1997) Mineral induction by immobilized phosphoproteins. *Bone* **21,** 305–311
38. Sun, Y., Lu, Y., Chen, S., Prasad, M., Wang, X., Zhu, Q., Zhang, J., Ball, H., Feng, J., Butler, W. T., and Qin, C. (2010) Key proteolytic cleavage site and full-length form of DSPP. *J. Dent. Res.* **89,** 498–503
39. von Marschall, Z., and Fisher, L. W. (2010) Dentin sialophosphoprotein (DSPP) is cleaved into its two natural dentin matrix products by three isoforms of bone morphogenetic protein-1 (BMP1). *Matrix Biol.* **29,** 295–303
40. Zhu, Q., Prasad, M., Kong, H., Lu, Y., Sun, Y., Wang, X., Yamoah, A., Feng, J. Q., and Qin, C. (2012) Partial Blocking of mouse DSPP processing by substitution of Gly^{451}-Asp^{452} bond suggests the presence of secondary cleavage site(s). *Connect. Tissue Res.* **53,** 307–312
41. Prasad, M., Zhu, Q., Sun, Y., Wang, X., Kulkarni, A., Boskey, A., Feng, J. Q., and Qin, C. (2011) Expression of dentin sialophosphoprotein in non-mineralized tissues. *J. Histochem. Cytochem.* **59,** 1009–1021
42. Sun, Y., Lu, Y., Chen, L., Gao, T., D'Souza, R., Feng, J. Q., and Qin, C. (2011) DMP1 processing is essential to dentin and jaw formation. *J. Dent. Res.* **90,** 619–624
43. Baba, O., Qin, C., Brunn, J. C., Jones, J. E., Wygant, J. N., McIntyre, B. W., and Butler, W. T. (2004) Detection of dentin sialoprotein in rat periodontium. *Eur. J. Oral. Sci.* **112,** 163–170
44. Martin, D. M., Hallsworth, A. S., and Buckley, T. (1978) A method for the study of internal spaces in hard tissue matrices by SEM, with special reference to dentine. *J. Microsc.* **112,** 345–352
45. Feng, J. Q., Ward, L. M., Liu, S., Lu, Y., Xie, Y., Yuan, B., Yu, X., Rauch, F., Davis, S. I., Zhang, S., Rios, H., Drezner, M. K., Quarles, L. D., Bonewald, L. F., and White, K. E. (2006) Loss of DMP1 causes rickets and osteomalacia and identifies a role for osteocytes in mineral metabolism. *Nat. Genet.* **38,** 1310–1315
46. Qin, C., Baba, O., and Butler, W. T. (2004) Post-translational modifications of sibling proteins and their roles in osteogenesis and dentinogenesis. *Crit. Rev. Oral. Biol. Med.* **15,** 126–136
47. Sun, Y., Gandhi, V., Prasad, M., Yu, W., Wang, X., Zhu, Q., Feng, J. Q., Hinton, R. J., and Qin, C. (2010) Distribution of small integrin-binding ligand, N-linked glycoproteins (SIBLING) in the condylar cartilage of rat mandible. *Int. J. Oral. Maxillofac Surg.* **39,** 272–281